Imaging Soft Samples with the Atomic Force Microscope: Gelatin in Water and Propanol

Manfred Radmacher, Monika Fritz, and Paul K. Hansma
Department of Physics, University of California, Santa Barbara, California 93106 USA

ABSTRACT We have imaged mica coated with thin gelatin films in water, propanol, and mixtures of these two liquids by atomic force microscopy (AFM). The elastic modulus (Young's modulus) can be tuned from 20 kPa to more than 0.1 GPa depending on the ratio of propanol to water. The resolution is best in pure propanol, on the order of 20 nm, and becomes worse for the softer samples. The degradation in resolution can be understood by considering the elastic indentation of the gelatin caused by the AFM tip. This indentation becomes larger and thus the contact area becomes larger the softer the sample is. Therefore this study may be used to estimate the resolution to be expected with an AFM on other soft samples, such as cells. Nondestructive imaging was possible only by imaging at forces <1 nN. This was difficult to achieve in contact mode because of drift in the zero load deflection of the cantilever, supposedly caused by temperature drift, but straightforward in tapping mode.

INTRODUCTION

The atomic force microscope (AFM) (Binnig et al., 1986; Rugar and Hansma, 1990) has been proven to be a very useful tool in imaging biological samples like proteins, DNA, or even whole cells (Hansma and Hoh, 1994; Henderson, 1994; Radmacher et al., 1992). The ability to image in liquids, especially physiological buffers, makes it a unique tool to observe biological processes at a submicroscopic scale (Fritz et al., 1994; Radmacher et al., 1994b). Despite these results it is still a challenge to image soft materials like proteins or cells with the AFM in their native environment without fixation. One reason might be that the softness of biological samples usually makes it very difficult to image with high resolution without sample damage. Although the effect of sample softness on resolution and general performance of the AFM is understood in principle, to our knowledge no quantitative experimental analysis has been undertaken so far.

Recently the AFM has been used to image elastic properties (Maivald et al., 1991; Radmacher et al., 1993; Baselt et al., 1993). Analyzing force curves on these soft small biological objects showed that the instrumentational development had led to reliable determination of mechanical properties on the submicron scale (Hoh and Schoenenberger, 1994; Radmacher et al., 1994a; Tao et al., 1992; Weisenhorn et al., 1993).

Synthetic polymers have been characterized with the AFM by imaging in air (Aimé et al., 1994; Mamin and Rugar, 1992; Meyers et al., 1992). Recently, thin gelatin films were investigated with AFM in air (Haugstad et al., 1994). Here we report on measuring the elastic properties of gelatin under different environments. Gelatin is the denatured form of the structural protein collagen. Collagen is a triple helix, made of three single α-helices wrapped around each other. During denaturing the molecule is broken in smaller pieces and the triple helices are disrupted leaving only single helices of molecular weight between 20 and 100 kDa depending on preparation. Aqueous solutions of gelatin are in the sol phase at elevated temperatures (depending on concentration at 30°C or higher temperatures) and form gels on cooling. One major part of the gelation process is probably the formation of triple helices in the polymer matrix. (for review see Djabourov, 1988; Clark and Ross-Murphy, 1987).

The Young's moduli can be measured by AFM and thus the contact radius can be estimated. The contact area will naturally affect the obtainable resolution, so that best resolution can be achieved only on hard samples. AFM images were taken both in the conventional contact mode and in a novel tapping mode in liquids (Hansma et al., 1994; Putman et al., 1994). Resolution was slightly better in tapping mode at moderate sample softnesses and seemed to become worse at very small Young's moduli. The softest samples (in 50% propanol and pure water) were impossible to image in tapping mode. Images in contact mode could be obtained. In these cases the images recorded do not only reveal topographic features of the sample but are also affected by the sample softness. Therefore the comparison between both modes is not straightforward and might need further investigation.

MATERIALS AND METHODS

Sample preparation

Gelatin extracted from porcine skin was purchased from Sigma Chemical Co. (St. Louis, MO). A total of 50 mg of gelatin was dissolved in 1 ml of pure water and kept in a water bath at boiling temperature for 30 min. A small droplet (10 μl) of this solution was applied to a piece of freshly cleaved mica, which was mounted in a home-built spincoater. The spin-

Received for publication 10 January 1995 and in final form 14 April 1995.
Address reprint requests to Dr. Manfred Radmacher, Department of Physics, University of California, Santa Barbara, CA 93106. Tel.: 805-893-3999; Fax: 805-893-8315; E-mail: manfred@physics.ucsb.edu.
© 1995 by the Biophysical Society
0006-3495/95/07/264/07 $2.00

coater was already rotating (~3000 rpm) as the solution was applied to the substrate and was kept running for approximately 30 more seconds. Samples were always prepared freshly and used the same day. Usually the samples were exposed for ~30 min to ambient air before being mounted in the AFM where they were immersed with either pure water or propanol before starting to image.

Instrumentation

AFM was performed with a commercial instrument (Nanoscope III, Digital Instruments, Santa Barbara, CA). All imaging was performed with soft silicon nitride cantilevers with integrated pyramidal tips (200-μm-long and 12-μm-wide triangular cantilever, custom-made prototype cantilevers with so-called oxide sharpened tips, courtesy of Mark Wendman, Digital Instruments). The force constant was determined to be 25 mN/m by measuring the resonance frequency of the cantilever (Cleveland et al., 1993). All imaging was performed under liquids. Propanol was purchased from Aldrich (Milwaukee, WI), and water was deionized and filtered (Millipore Systems, Eugene, OR).

Imaging was performed in a glass fluid cell with ports so that the fluid in the chamber could be exchanged easily with the sample and the cantilever already mounted. All the data reported here were taken with the same sample and the same cantilever. We have observed the described results with several samples and several cantilevers but present here results of only one run to make the individual results comparable with each other.

The images were recorded either in the conventional contact mode or in a novel tapping mode developed recently (Hansma et al., 1994). In contact mode the deflection of the cantilever while touching and scanning the sample is monitored. Feedback electronics tries to adjust the sample height such that the cantilever deflection stays constant. Displaying the height at each sample position will create a topograph of the sample surface. In tapping mode the cantilever is vibrated externally. The amplitude of this oscillation of the tip will become smaller when the tip touches the surfaces. Therefore, feedback electronics trying to adjust the sample height such that the amplitude stays constant will trace the sample surface. Tapping mode largely reduces the amount of lateral forces usually present in the conventional contact mode. This has proven to be very successful with single adsorbed protein molecules (Radmacher et al., 1994b; Bezanilla et al., 1994). Another advantage is that tapping mode is not sensitive to drift of the cantilever. The cantilevers most often used in AFM (micromanufactured silicon nitride cantilevers) bend as a result of temperature changes (Radmacher et al., 1995). This bending will result in different free cantilever positions corresponding to different cantilever deflections. In contact mode the feedback electronics tries to keep the deflection constant, which will therefore lead to drift in the loading force.

Data analysis

Force curves were analyzed in the following way. A force curve on a hard sample has basically two linear regions, one where the cantilever deflection is constant (the tip is off the surface) and a sloped region where the tip is touching the surfaces and the deflection is proportional to the movement of the sample by the piezo. In the case of soft samples the deflection will be smaller as a result of sample indentation (see Fig. 1). By subtracting the measured deflection from the known response of the cantilever on a hard surface we can calculate the indentation (Fig. 1 *a*). For modeling the indentation we want to plot it as a function of the loading force and not as a function of the *z* movement of the piezo. The loading force is given by the measured cantilever deflection multiplied by the force constant of the cantilever (Fig. 1 *b*). The experimental data can be modeled by the so-called Hertz model as described below. It turns out that a log-log plot of the indentation as a function of the loading force is very helpful in analyzing the data (Fig. 1 *c*).

Force versus indentation curves can be modeled by the Hertz model (Hertz, 1881) describing the elastic deformation of two surfaces touching under load. Two different geometries seem to be appropriate to describe the

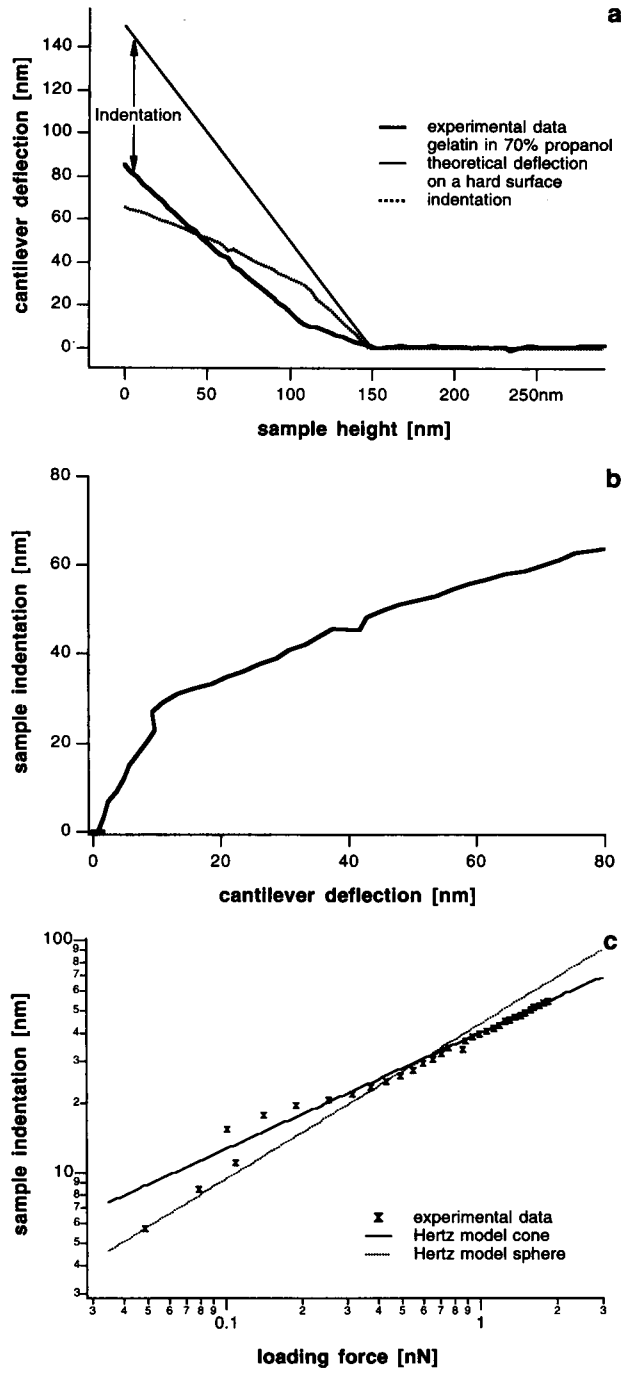

FIGURE 1 (a) Force curves (approach traces only) taken on a gelatin sample immersed in 70% propanol (*thick trace*) and on a very hard sample (*thin trace*). Because of elastic indentation on the soft sample the same piezo movement results in a smaller cantilever deflection than on the hard sample. The difference between both curves is the indentation (*dotted trace*). For modeling the elastic indentation it is necessary to plot the indentation as a function of the applied loading force. The loading force is given by the obtained cantilever deflection multiplied by its force constant (*b*). As will be described below in more detail a convenient way of comparing the model and the data is plotting both on a log-log scale (*c*). (*c*) shows the indentation versus loading force (same as in *b*) and compares it with the prediction of the Hertz model for two different geometries: a sharp cone (opening angle 30°) and a sphere (radius of curvature 20 nm) indenting in a soft sample. In both cases the Poisson ratio was chosen to be 0.5 and the Young's modulus was adjusted to give a good fit (0.7 MPa in the case of the cone and 0.3 MPa in the case of the sphere).

AFM tip and the sample: either a sphere of radius R or a cylindrical cone of opening angle α indenting a planar soft sample. For these two cases the Hertz model predicts a different functional relation between the loading force needed to create a given indentation. In the case of an infinitely hard sphere of radius R (AFM tip) touching a soft planar surface the Hertz model gives the following relation between the loading force F and the indentation δ:

$$F_{\text{sphere}} = \frac{4}{3}\frac{E}{(1-\nu)}\sqrt{R}\delta^{3/2}, \quad (1)$$

where E is the Young's modulus and ν is the Poisson ratio of the soft material. In the case of a cylindrical cone indenting a soft material the relationship between loading force and resulting indentation is as follows:

$$F_{\text{cone}} = \frac{\pi}{2}\frac{E}{(1-\nu)}\tan(\alpha)\delta^2, \quad (2)$$

where α is the opening angle of the cone. We will show below which model is more appropriate in our case. These two functions will appear as a line with a different slope on a log-log plot (see Fig. 1 *c*).

In the case of a very hard sample the movement z of the piezo while in contact will lead to a deflection d of the cantilever that is identical to z: $d = z$. In the case of a soft sample the same movement z will lead to a smaller deflection of the cantilever as a result of an elastic indentation δ: $z = d + \delta$. The loading force F is proportional to the deflection d of the cantilever and the force constant k of the cantilever and can be written as

$$F = k * d = k * (z - \delta). \quad (3)$$

In a force curve we measure the deflection as a function of the z movement of the piezo. Equation 3 can be used to calculate indentation versus force relations from the measured data set. These indentation versus force curves can then be analyzed by modeling the elastic indentation by using either Eq. 1 or 2, as will be discussed below.

RESULTS

Fig. 1 shows a force curve taken on gelatin immersed in 70% propanol. In Fig. 1 *a* the measured force curve (thick trace) together with the theoretical force curve taken on a hard sample (thin trace) is shown. The difference between the two is the indentation on the soft sample. This indentation is plotted versus the cantilever deflection in Fig. 1 *b*. The cantilever deflection is proportional to the loading force, related by the force constant of the cantilever. Fig. 1 *c* shows the deflection plotted as a function of the loading force on a log-log scale. Also shown in this graph is the theoretical indentation as predicted by the Hertz model for the two different geometries mentioned above: a sphere and a cone indenting a flat soft surface. Parameters used are a Young's modulus of 0.7 MPa in the case of the cone and 0.3 MPa in the case of the sphere, a Poisson ratio of 0.5, tip radius of 20 nm, and opening angle of 30°. The tip radius is a typical value known from the tip broadening of small structures like proteins (Karrasch et al., 1993; Yang et al., 1994). The opening angle was measured by scanning a calibration grating showing square pits with very steep walls (Digital Instruments) (for tip convolution and image reconstruction see Keller and Franke, 1993). The apparent tilt of these walls is a good estimate for the opening angle of the tips used. The measured value of a tip from the same wafer as the experimental tip was 29–35°. In the case of our experiment the elastic indentation is modeled more precisely by a cone compared with a sphere indenting a soft sample. This might be because the indentations are large compared with the radius of curvature of the tip at the very end (a typical value is 20 nm). At smaller indentations the tip might be better approximated by a sphere (Radmacher et al., 1994a; see also Fig. 1 *c* at smaller indentations).

Fig. 2 shows force curves taken on the same gelatin sample in different liquids. The elastic properties change while the gelatin is immersed in pure water, propanol, or mixtures of the two; gelatin becomes softer and softer as the water content in propanol is increased from 0% to 15%, 30%, 50%, and finally pure water. The same motion of the piezo leads to a smaller deflection as a result of elastic indentation of the sample. By replacing the water with propanol the gelatin becomes hard again. This transition was reversible and could be made several times. After replacing the fluids there is a fast change in the elastic properties that is too fast for detecting with our instrumentation followed by a slow drift in the elastic properties on the time scale of hours. Therefore force curves were taken just before and after taking the images shown below to obtain accurate numbers of the actual softness of the sample. These values for the elastic properties were reproducible within 20%. We did not wait until this slow drift in elastic properties has settled down as determining accurately the steady-state elastic properties in a given environment was not the issue of this study. We were interested in tuning these properties and documenting the obtainable resolution at a given, measurable sample softness. This remark applies especially to the samples immersed in water, for which not only a slow drift in sample softness occurred but also a slow dissolving of the gelatin on an hour time scale was visible. In this sense tuning of the elastic properties was reversible only when the sample had not been immersed in water for a long time (more than 2 h).

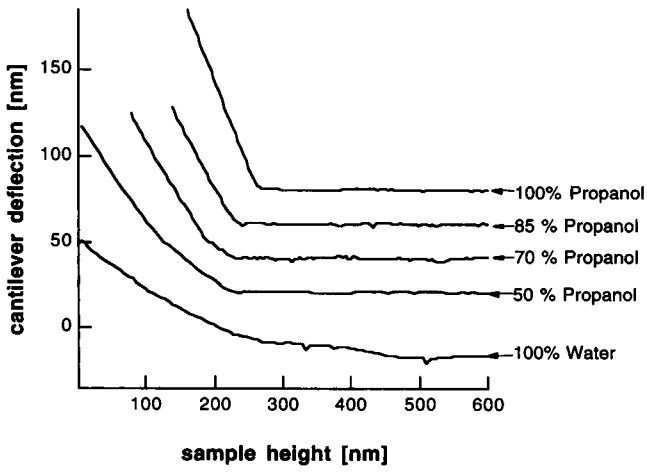

FIGURE 2 Force curves of thin gelatin films in different media. The curve in propanol is almost indistinguishable from the force curve taken on a hard substrate. The more water is added to the propanol the softer the gelatin appears to be. These curves will be analyzed below to get values for the Young's modulus.

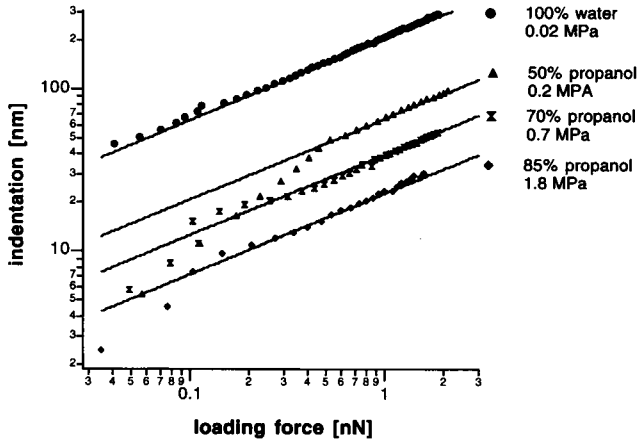

FIGURE 3 Measured indentation as a function of loading force. These curves are extracted from the force curves of Fig. 1 as described in the text. Also shown are the predictions of the Hertz model used to determine the Young's modulus of each sample (*solid lines*). The Young's modulus of the gelatin has been determined to be larger than 0.1 GPa in 100% propanol, 1.8 MPa in 85% propanol, 0.7 MPa in 70% propanol, 0.2 MPa in 50% propanol, and 0.02 MPa in pure water.

Fig. 3 shows the indentation as a function of loading force obtained by applying Eq. 3 to the data shown in Fig. 2 plotted on a log-log scale. Each data set is shown with a theoretical trace for a cone indenting a flat surface, adjusting the Young's modulus to give a good fit of data and theory. The opening angle and the Poisson ratio are chosen as above (30° and 0.5, respectively).

Fig. 4 shows two images of the same area imaged in pure water (*a*) and pure propanol (*b*). In water, only the global changes of the topography at a micrometer scale are visible. In propanol, details down to a scale of ~20 nm are visible. The image in water (Fig. 4 *a*) was possible only after increasing the force to ~2 nN. At this loading force the indentation of the tip is already 40 nm (see Fig. 3). This is approximately the height of the observed, small scale corrugations in Fig. 4 *b*. The global changes of topography correlate well in both images. However, all the small scale details visible in propanol (Fig. 4 *b*) are not visible in water any more because of the large elastic indentation of the AFM tip into the gelatin. Therefore we conclude that the elastic properties of the sample, especially while immersed in water, play a large role in its appearance.

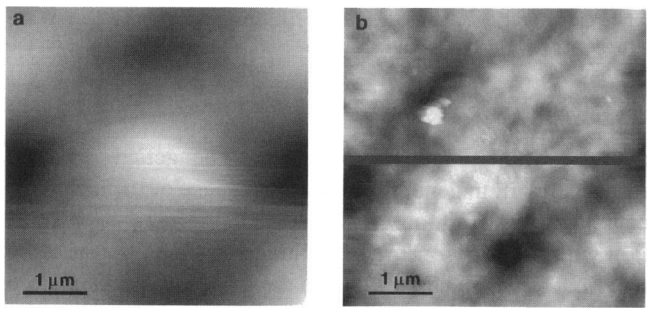

FIGURE 4 The same area of a thin film of gelatin imaged in contact mode in pure water (*a*) and propanol (*b*). In water only the global surface structure is visible with a resolution on the order of one micrometer. In propanol much more detail is visible resulting in a resolution on the order of 20 nm. A few scan lines in the center portion of the image are missing due to drift in the system and liftoff of the tip off the sample. In propanol the loading force was tried to minimize giving the best resolution with the drawback of eventual liftoff of the tip (<0.4 nN). In water the loading force has to be increased to ~2 nN to achieve any contrast. Note that the *z*-range is different in the two images: 300 nm for *a* and 80 nm for *b*.

Fig. 5 shows a series of images recorded in contact mode where imaging was performed in pure propanol and mixtures of propanol with water. With decreasing softness of the sample the resolution decreases also. At 85% propanol most of the features on a 500-nm scale have disappeared (Fig. 5, *a-c*). The same happens on an even larger scale at 50% propanol (Fig. 5, *d-g*). In pure water the resolution is poor (Fig. 5 *h*) but can be restored by going back to pure propanol (Fig. 5 *i*).

During the course of this experiment we also recorded a series of images in tapping mode (Fig. 6). These data were recorded with the same tip on the same sample directly after the images in contact mode had been taken. Therefore the data can be compared without worrying about variations of sample preparation or of the tip shape. At high propanol concentration the resolution is comparable or even better than in contact mode (Fig. 6, *a-c*; 100, 95, and 85% propanol, respectively). At 70% propanol (Fig. 6 *f*) the resolution is already poor. At even higher water concentration (50% propanol and pure water) imaging was impossible in tapping mode although imaging was still possible in contact mode (Figs. 5, *g* and *h*, and 4 *a*). (Please note that in Fig. 6 the scan size is larger in *c-f* compared with *a* and *b*).

DISCUSSION

One possible artifact in determining the elastic modulus of the gelatin films has to be discussed first. Because gelatin swells in water the gelatin films will have different thicknesses depending on the water content of the liquid in which they are immersed. If the thickness of the film is on the order of the applied indentations, one might expect that the AFM tip also feels the underlying substrate while indenting and that therefore the sample will appear to be stiffer than it actually is. This should result in an indentation versus loading force curve with a changing slope. At low loading forces a measurable indentation can be achieved and at higher loading forces the indentation will eventually become constant when the thin film is entirely compressed. We did not observe this behavior nor did we see any deviation of the Hertzian behavior at higher loading forces. To strengthen this point we measured the thickness of the gelatin films by scratching them very gently with a scalpel and imaging the scratch with the AFM. The films had been rinsed thoroughly with propanol after scratching and were imaged in air. The measured thickness was ~130 nm. This thickness has to be compared with the maximum indentation in the case of the stiff samples (propanol), which was 15 nm. Therefore we can conclude that our measurements

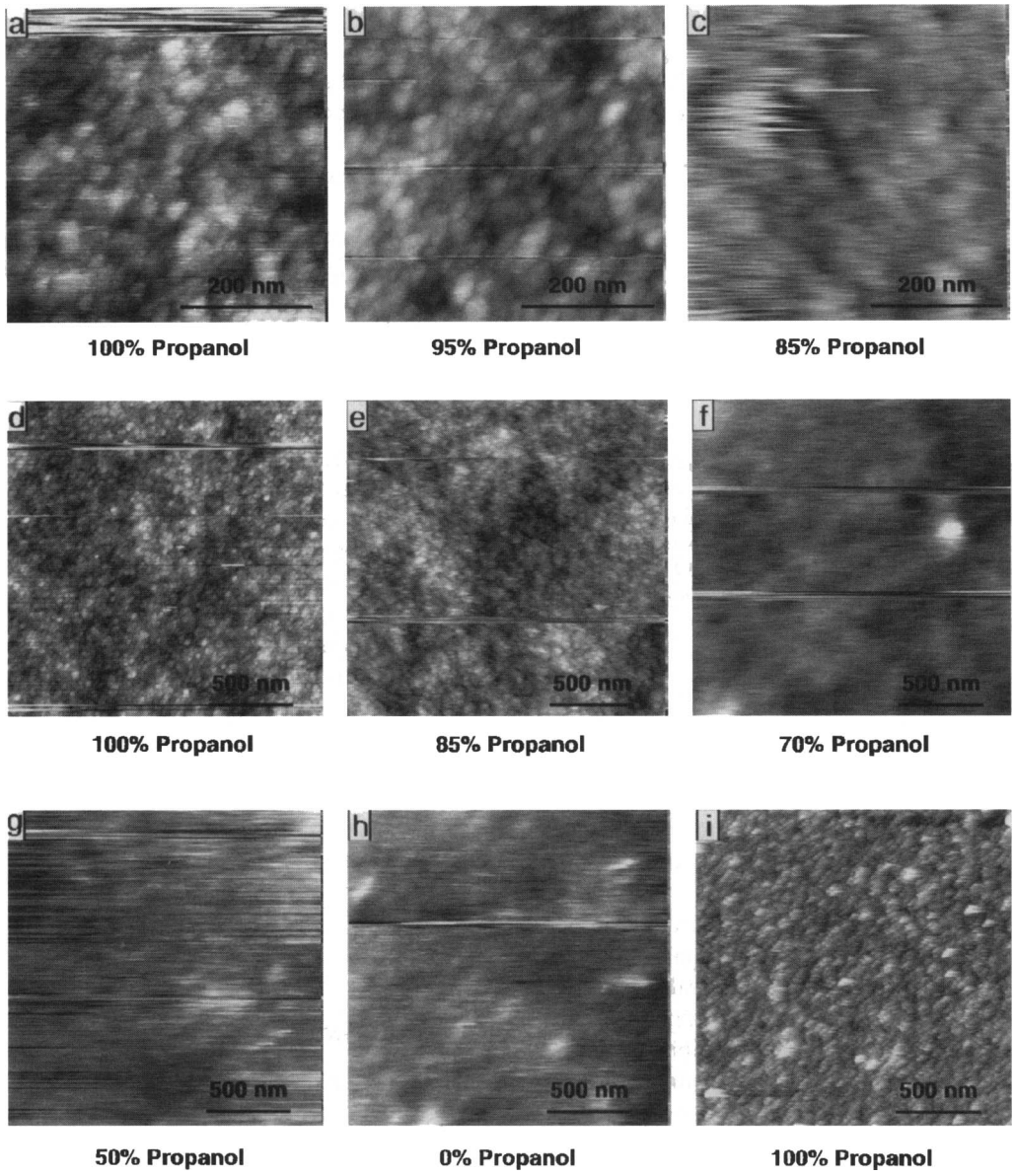

FIGURE 5 Thin gelatin films imaged with the AFM in contact mode in different media. The top row shows an image at 500 nm scan size in pure propanol (*a*), 95% propanol (*b*), and 85% propanol (*c*). The resolution decreases slowly while the sample becomes softer and softer. Images *d* through *h* show the same sample in pure propanol, in 85, 70, and 50% propanol, and in pure water (image size is 2 μm). By immersing the sample in propanol again (*i*) the original image can be restored. (imaging forces < 0.4 nN).

were not affected by the thickness of the gelatin films and the elastic moduli obtained are the moduli of the sample itself.

Fig. 7 shows the radius of contact of an AFM tip as estimated by the Hertz model using the two interesting geometries together with the experimentally obtained resolution as a function of the Young's modulus of the sample. The resolution was estimated by measuring the distance between two distinct, nearby features in the images. Parameters used for the model predictions are a Poisson ratio of 0.5, a tip radius of 20 nm for the sphere model, and an opening angle of 30° for the cone model. As the radius of contact was estimated by assuming a Hertzian contact between a very hard tip and a soft planar sample, this will give a lower estimate of the resolution. The actual obtained resolution will in general be poorer, because of the influence of topography. Tapping mode shows slightly higher resolution with the harder samples in this experiment. It has to be mentioned that all samples, even the gelatin in propanol, are very soft samples, compared with the substrates usually used in AFM; glass for instance has a Young's modulus of 70 GPa.

We have presented here only data taken on the same sample and with the same cantilever and tip. As the resolution obtainable with AFM will depend on the tip geometry, e.g., the tip radius, this was necessary for obtaining comparable results. However, we found out that there is not much variation in the tips while using the same type of

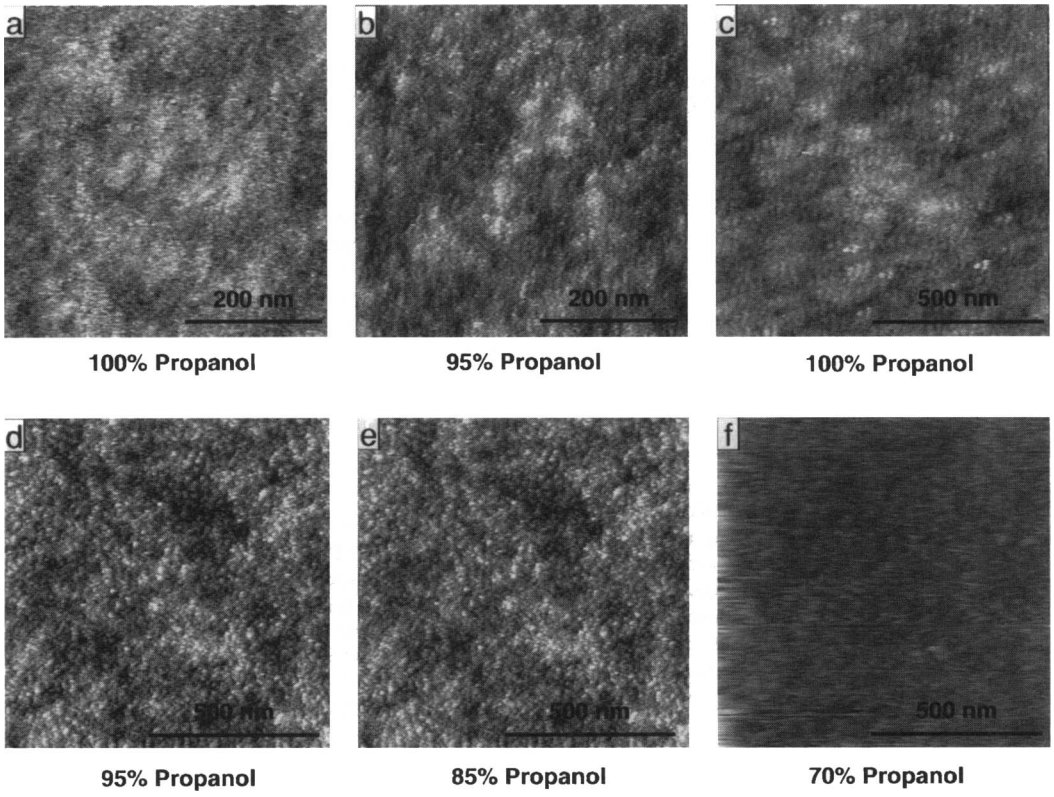

FIGURE 6 Thin gelatin films imaged in tapping mode. The water concentration has been increased gradually from 0% (pure propanol) (*a*) to 70% water (*f*). High resolution images are possible at low water concentrations, corresponding to a Young's modulus of the sample larger than 2 MPa, but decreases rapidly for samples with ≤30% water.

cantilevers from the same batch. Different types of cantilevers might lead to quantitatively slightly different results, but the qualitative trend should be the same. There was some variation in the sample preparations resulting in gelatin films with elastic properties deviating by a factor of 2 under the same conditions. However, correlating the measurable elastic properties with the obtained resolution was reproducibly independent of the cantilever used.

The very soft samples could be imaged only at high loading force, where no topographic but more elastic imaging is performed. So far, tapping mode has been optimized for low loading forces. Low force imaging was not possible in either contact or tapping mode on the softest samples. High forces (>1 nN) in contact mode did yield images, but these are probably highly influenced by localized elasticity rather than topography.

In contact mode, loading forces have to be minimized always by adjusting the scan parameters. This is a result of the fact that silicon nitride cantilevers bend as a result of temperature fluctuations. Therefore the unloaded cantilever will be more or less bent depending on the temperature. This means that the feedback of the atomic force microscope will actually change the loading force in trying to keep the deflection signal constant. This drift in loading force can be a few nanonewtons per minute and will eventually settle down after hours of equilibration. As this was not a possibility in our case (we were imaging the same sample on the same day in seven different liquids) we constantly had to adjust the set point. This leads eventually to lift-off of the cantilever as is visible by the missing scan lines in Figs. 4 *b* and 5. In tapping mode the feedback loop looks at the high frequency oscillatory response of the cantilever. The slow drifts in cantilever bending will not be detected and thus not lead to any drift in the loading force. As visible in the tapping mode images, no adjustment of the imaging parameters was necessary and therefore no scan lines are missing.

The softer samples were also hard or impossible to image without any damage. This gives practical estimates for the capability of the AFM to image soft samples like polymers, biological material, and cells of comparable softness.

CONCLUSIONS

We show here a quantitative correlation between the resolution and the softness of the material while imaging soft samples with the AFM. Depending on the tip radius and the loading force a lower limit for the resolution can be estimated by calculating the contact radius assuming a Hertzian contact.

We especially thank Mark Wendman (Digital Instruments) for providing prototype Si_3N_4 cantilever tips. We thank H.-J. Butt and Roger Proksch for helpful discussions.

This work was supported by a grant from the Materials Research Division

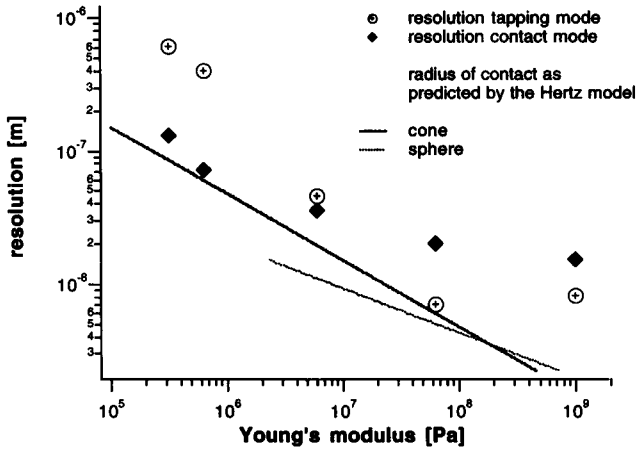

FIGURE 7 Estimated radius of the contact area shown as a solid line as a function of the Young's modulus of the material under investigation. Experimental resolution obtained in contact and tapping mode on gelatin samples is shown with data points. Note that the experimental resolution is bounded by the radius of the contact area: the experimental points, in general, lie above the solid line. The contact area is estimated assuming an Hertzian contact of two different geometries: either an cone of opening angle 30° or a sphere of radius 20 nm. (Note that the model of a sphere touching a planar surface only makes sense for small contact areas, i.e. smaller than the radius of the sphere. Therefore the theoretical line for a sphere covers only part of the range of the graph.)

of the National Science Foundation under grant NSF-DMR 9221781 (M.R. and P.K.H.) and the Deutsche Forschungsgemeinschaft (M.F.). Equipment was supplied by Digital Instruments.

REFERENCES

Aimé, J. P., Z. Elkaakour, C. Odin, T. Bouhacina, D. Michel, J. Curély, and A. Dautant. 1994. Comments on the use of the force mode in atomic force microscopy for polymer films. *J. Appl. Phys.* 76:754–762.

Baselt, D. R., S. M. Clark, M. G. Youngquist, C. F. Spence, and J. D. Baldeschieler. 1993. Digital signal processor control of scanned probe microscopes. *Rev. Sci. Instrum.* 64:1874–1882.

Bezanilla, M., B. Drake, E. Nudler, M. Kashlev, P. K. Hansma, and H. G. Hansma. 1994. Motion and enzymatic degradation of DNA in the atomic force microscope. *Biophys. J.* 67:1–6.

Binnig, G., C. F. Quate, and C. Gerber. 1986. Atomic force microscope. *Phys. Rev. Lett.* 56:930.

Clark, A. H., and S. B. Ross-Murphy. 1987. Structural and mechanical properties of biopolymer gels. *Adv. Polymer Sci.* 83:57–192.

Cleveland, J. P., S. Manne, D. Bocek, and P. K. Hansma. 1993. A nondestructive method for determining the spring constant of cantilevers for scanning force microscopy. *Rev. Sci. Instrum.* 64:403–405.

Djabourov, M. 1988. Architecture of gelatin gels. *Contemp. Phys.* 29: 273–297.

Fritz, M., M. Radmacher, and H. E. Gaub. 1994. Granula motion and membrane spreading during activation of human platelets imaged by atomic force microscopy. *Biophys. J.* 66:1328–1334.

Hansma, P. K., J. P. Cleveland, M. Radmacher, D. A. Walters, P. E. Hillner, M. Bezanilla, M. Fritz, D. Vie, H. G. Hansma, C. B. Prater, J. Massie, L. Fukunaga, J. Gurley, and V. Elings. 1994. Tapping mode atomic force microscopy in liquids. *Appl. Phys. Lett.* 64:1738–1740.

Hansma, H. G., and J. H. Hoh. 1994. Biomolecular imaging with the atomic force microscope. *Annu. Rev. Biophys. Biophys. Chem.* 23: 115–139.

Haugstad, G., W. L. Gladfelter, E. B. Weberg, R. T. Weberg, and T. D. Weatherill. 1994. Probing bioploymers with scanning force methods: adsorption, properties, and transformations of gelatin on mica. *Langmuir.* 10:4295–4306.

Henderson, E. 1994. Imaging of living cells by atomic force microscopy. *Prog. Surface Sci.* 46:39–60.

Hertz, H. 1881. Über den Kontakt elastischer Körper. *J. Reine Angew. Mathematik.* 92:156.

Hoh, J. H., and C.-A. Schoenenberger. 1994. Surface morphology and mechanical properties of MDCK monolayers by atomic force microscopy. *Biophys. J.* 107:1105–1114.

Karrasch, S., M. Dolder, F. Schabert, J. Ramsden, and A. Engel. 1993. Covalent binding of biological samples to solid supports for scanning probe microscopy in buffer solution. *Biophys. J.* 65:2437–2446.

Keller, D. J., and F. S. Franke. 1993. Envelope reconstruction of probe microscope images. *Surface Sci.* 294:409–412

Maivald, P., H. J. Butt, S. A. C. Gould, C. B. Prater, B. Drake, J. A. Gurley, V. B. Elings, and P. K. Hansma. 1991. Using force modulation to image surface elasticities with the AFM. *Nanotechnology.* 2:103–106.

Mamin, H. J., and D. Rugar. 1992. Thermomechanical writing with an atomic force microscope. *Appl. Phys. Lett.* 61:1003–1005.

Meyers, G. F., B. M. DeKoven, and J. T. Seitz. 1992. Is the molecular surface of polystyrene glassy? *Langmuir.* 8:2330–2335.

Putman, C. A. J., K. O. van der Werf, B. G. De Grooth, N. F. Van Hulst, and J. Greve. 1994. Viscoelasticity of living cells allows high-resolution imaging by tapping mode atomic force microscopy. *Biophys. J.* 67: 1749–1753.

Radmacher, M., J. P. Cleveland, and P. K. Hansma. 1995. Improvement of thermally induced bending of cantilevers used for AFM. *Scanning.* In press.

Radmacher, M., M. Fritz, J. P. Cleveland, D. R. Walters, and P. K. Hansma. 1994a. Imaging adhesion forces and elasticity of lysozyme adsorbed on mica by atomic force microscopy. *Langmuir.* 10: 3809–3814.

Radmacher, M., M. Fritz, H. G. Hansma, and P. K. Hansma. 1994b. Direct observation of enzyme activity with the atomic force microscope. *Science.* 265:1577–1579.

Radmacher, M., R. W. Tillmann, M. Fritz, and H. E. Gaub. 1992. From molecules to cells: imaging soft samples with the AFM. *Science.* 257: 1900–1905.

Radmacher, M., R. W. Tillman, and H. E. Gaub. 1993. Imaging viscoelasticity by force modulation with the atomic force microscope. *Biophys. J.* 64:735–742.

Rugar, D., and P. K. Hansma. 1990. Atomic force microscopy. *Phys. Today* 43:23–30.

Tao, N. J., N. M. Lindsay, and S. Lees. 1992. Measuring the microelastic properties of biological materials. *Biophys. J.* 63:1165–1169.

Weisenhorn, A. L., M. Khorsandi, S. Kasas, V. Gotozos, M. R. Celio, and H. J. Butt. 1993. Deformation and height anomaly of soft surfaces studied with the AFM. *Nanotechnology.* 4:106–113.

Yang, J., J. Mou, and Z. Shao. 1994. Molecular resolution atomic force microscopy of soluble proteins in solution. *Biochim. Biophys. Acta.* 1199:105–114.